Cantor dust zone plates

Vicente Ferrando,[1,2] **Arnau Calatayud,**[1] **Fernando Giménez,**[3]
Walter D. Furlan,[2] **and Juan A. Monsoriu**[1,*]

[1]*Centro de Tecnologías Físicas, Universitat Politècnica de València, 46022 Valencia, Spain*
[2]*Departamento de Óptica, Universitat de València, 46100 Burjassot, Spain*
[3]*I.U. Matemática Pura y Aplicada, Universitat Politècnica de València, 46022 Valencia, Spain*
[*]*jmonsori@fis.upv.es*

Abstract: In this paper we use the Cantor Dust to design zone plates based on a two-dimensional fractal for the first time. The pupil function that defines the coined Cantor Dust Zone Plates (CDZPs) can be written as a combination of rectangle functions. Thus CDZPs can be considered as photon sieves with rectangular holes. The axial irradiances produced by CDZPs of different fractal orders are obtained analitically and experimentally, analyzing the influence of the fractality. The transverse irradiance patterns generated by this kind of zone plates has been also investigated.

© 2013 Optical Society of America

OCIS codes: (050.1940) Diffraction; (050.1970) Diffractive optics.

References and links

1. A. Siemion, A. Siemion, M. Makowski, J. Suszek, J. Bomba, A. Czerwiski, F. Garet, J.-L. Coutaz, and M. Sypek, "Diffractive paper lens for terahertz optics," Opt. Lett. **37,** 4320–4322 (2012).
2. A. Sakdinawat and Y. Liu, "Soft-x-ray microscopy using spiral zone plates," Opt. Lett. **32,** 2635–2637 (2007).
3. G. Saavedra, W. D. Furlan, and J. A. Monsoriu, "Fractal zone plates," Opt. Lett. **28,** 971–973 (2003).
4. J. A. Davis, L. Ramirez, J. A. Rodrigo Martín-Romo, T. Alieva, and M. L. Calvo, "Focusing properties of fractal zone plates: experimental implementation with a liquid-crystal display," Opt. Lett. **29,** 1321–1323 (2004).
5. J. A. Monsoriu, G. Saavedra, and W. D. Furlan, "Fractal zone plates with variable lacunarity," Opt. Express **12,** 4227–4234 (2004), http://www.opticsinfobase.org/oe/abstract.cfm?uri=oe-12-18-4227.
6. D. Hai-Tao, W. Xin, and X. Ke-Shu, "Focusing properties of fractal zone plates with variable lacunarity: experimental studies based on liquid crystal on silicon," Chinese Phys. Lett. **22,** 2851–2854 (2005).
7. W. D. Furlan, G. Saavedra, and J. A. Monsoriu, "White-light imaging with fractal zone plates," Opt. Lett. **32,** 2109–2111 (2007).
8. X. Ge, Z. Wang, K. Gao, D. Wang, Z. Wu, J. Chen, Z. Pan, K. Zhang, Y. Hong, P. Zhu, and Z. Wu, "Use of fractal zone plates for transmission x-ray microscopy," Anal. Bioanal. Chem. **404,** 1303–1309 (2012).
9. L. J. Janicijevic, "Diffraction characteristics of square zone plates," J. Opt. **13,** 199–206 (1982).
10. J. Alda, J. M. Rico-García, F. J. Salgado-Remacha, and L. M. Sanchez-Brea, "Diffractive performance of square Fresnel zone plates," Opt. Commun. **282,** 3402–3407 (2009).
11. A. Calatayud, V. Ferrando, F. Giménez, W. Furlan, G. Saavedra, and J. Monsoriu, "Fractal square zone plates," Opt. Commun. **286,** 42–45 (2013).
12. L. Kipp, M. Skibowski, R. L. Johnson, R. Berndt, R. Adelung, S. Harm, and R. Seemann, "Sharper images by focusing soft x-rays with photon sieves," Nature (London) **414,** 184–188 (2001).
13. Q. Cao and J. Jahns, "Focusing analysis of the pinhole photon sieve: individual far-field model," J. Opt. Soc. Am. A **19,** 2387–2393 (2002).
14. C. Xie, X. Zhu, H. Li, L. Shi, and Y. Wang, "Feasibility study of hard-x-ray nanofocusing above 20 keV using compound photon sieves," Opt. Lett. **35**, 4048–4050 (2010).
15. C. Xie, X. Zhu, H. Li, L. Shi, Y. Hua, and M. Liu, "Toward two-dimensional nanometer resolution hard X-ray differential-interference-contrast imaging using modified photon sieves," Opt. Lett. **37**, 749–751 (2012).
16. G. Andersen, "Membrane photon sieve telescopes," Appl. Phys. **49**, 63916394 (2010).
17. F. Giménez, J. A. Monsoriu, W. D. Furlan, and A. Pons, "Fractal photon sieve," Opt. Express **14,** 11958–11963 (2006), http://www.opticsinfobase.org/oe/abstract.cfm?uri=oe-14-25-11958.
18. F. Giménez, W. D. Furlan, and J. A. Monsoriu, "Lacunar fractal photon sieves," Opt. Commun. **277,** 1–4 (2007).

#181234 - $15.00 USD Received 5 Dec 2012; revised 14 Jan 2013; accepted 14 Jan 2013; published 28 Jan 2013
(C) 2013 OSA

19. B. Zhang and D. Zhao, "Square Fresnel zone plate with spiral phase for generating zero axial irradiance," Opt. Lett. **35**, 1488–1490 (2010).
20. F. J. González, J. Alda, B. Ilic, and G. D. Boreman, "Infrared antennas coupled to lithographic Fresnel zone plate lenses," Appl. Opt. **43**, 6067–6073 (2004).
21. L. Kelemen, S. Valkai, and P. Ormos, "Parallel photopolymerisation with complex light patterns generated by diffractive optical elements," Opt. Express **15**, 14488–14497 (2007), http://www.opticsinfobase.org/oe/abstract.cfm?uri=oe-15-22-14488.

1. Introduction

A renewed interest in focusing diffractive optical elements has been experienced by the scientific community in the last years because these elements are essential in image forming setups not only used in the visible range, but also in THz optics [1] or in X-ray microscopy [2]. Following this trend, our group introduced a new type of image-forming structure: the Fractal Zone Plate (FZP) [3] which is based on the one-dimensional Cantor Set. It has been proved theoretically [3] and experimentally [4] that under monochromatic plane wave illumination, a FZP produces multiple foci along the optical axis. The internal structure of each focus exhibits a characteristic fractal structure that reproduces the self-similarity of the originating FZP. The number of foci and their relative amplitude can be modified with the FZP design [5, 6]. It has been shown that this property can be profited in image forming systems to obtain an enhancement of the depth of field [7, 8].

Square zone plates (SZPs) [9, 10] are another kind of interesting diffractive optical elements which can be obtained as the combination of two linear Fresnel zone plates and produces a focalization pattern with a cross-like irradiance distribution. Based on the SZP, Fractal Rectangular Zone Plates (FSZPs), i.e., zone plates with a fractal distribution of square zones, have been recently introduced providing a main focal volume containing a self-similar sequence of cross-shaped patterns [11].

On the other hand, a Photon Sieve (PS) [12, 13] is another promising diffractive optical element that is based on a classical Fresnel zone plate. It is constructed by substitution of the transparent areas in it by a great number of non overlapping circular holes of different sizes. PSs have been proposed for hard-x-ray focusing, in the high energy region above 20 keV [14] and also used in two-dimensional hard-x-ray differential-interference-contrast imaging [15]. In addition, they have been recently employed in prototypes of primary lenses for lightweight space telescopes [16]. The principal characteristic of a PS is that it improves the resolution of a conventional zone plate. Moreover, when a fractal distribution of holes is considered an extended depth of field is also obtained [17, 18].

In this work we present the Cantor Dust Zone Plate (CDZP) as combination of the concepts of FSZP and PS. We have replaced the transparent square zones of a FSZP by a set of rectangular holes spatially distributed according to a two dimensional fractal known as Cantor Dust. To our knowledge, CDZPs are the first family of diffractive lenses designed with a two-dimensional fractal, improving the performance of FSZPs mainly on two aspects: 1) A CDZP has not connected regions so it can be fabricated in a single surface without any substrate. 2) The distribution of holes produces the apodization that improves the diffraction efficiency of a FSZP.

2. Cantor dust zone plate design

A CDZP is based on a 2D fractal which is geometrically constructed as shown in Fig. 1(a). Starting from two elements, $S = 0$ and $S = 1$, called the initiator and the generator respectively, the next higher order elements $S = 2, 3...$ are constructed sequentially by replacing every white square in the previous stage by the generator ($S = 1$). Mathematically the fractal Cantor Dust

#181234 - $15.00 USD Received 5 Dec 2012; revised 14 Jan 2013; accepted 14 Jan 2013; published 28 Jan 2013
(C) 2013 OSA

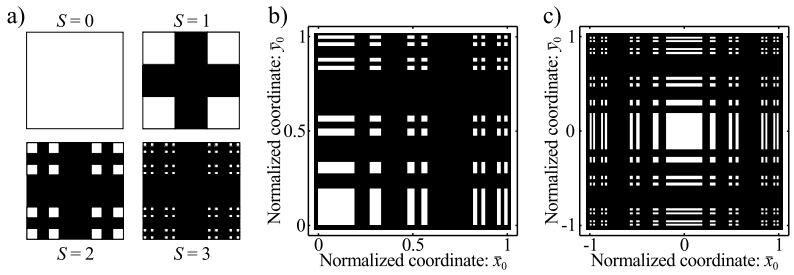

Fig. 1. (a) Geometrical construction of the Cantor Dust distribution up to third order. (b) Cantor dust varying the distribution sides quadratically with respect to the transverse coordinates. (c) Pupil function $q(\bar{x}_0,\bar{y}_0)$ —Eq. (2)— obtained from the order $S=3$ Cantor Dust distribution.

distribution can be generated by using an array of binary elements. Starting from the 1×1 array seed, $t_0=[1]$, the next higher fractal order is constructed by applying to each element the following transformation rules:

$$[1]\rightarrow\begin{bmatrix}1&0&1\\0&0&0\\1&0&1\end{bmatrix}\qquad\text{and}\qquad[0]\rightarrow\begin{bmatrix}0&0&0\\0&0&0\\0&0&0\end{bmatrix}\quad.\tag{1}$$

After an arbitrary number of iterations, S, a binary array, t_S, is obtained with $3^S\times 3^S$ elements. The array elements of t_S will be referred as $t_{Sjj'}$, where j and j' take values from 1 to 3^S. With this encoding, "1" represents a white square and "0" represents a black one.

From this geometrical representation, a CDZP can be constructed as a photon sieve constituted by an array of rectangular transparent holes, white squares, distributed along the squared transverse coordinates —see Fig. 1(b)—. Then, to obtain the corresponding pupil function two reflection (mirror) symmetries are applied being the mirror lines the coordinate axes —see Fig. 1(c)—. Note that a CDZP can be considered as a FSZP [11] where the square rings are replaced by a set of rectangular holes. Mathematically, the pupil function which represents a CDZP can be written as:

$$q(\bar{x}_0,\bar{y}_0)=\sum_{j=1}^{N}\sum_{j'=1}^{N}t_{Sjj'}RECT_j(\bar{x}_0)RECT_{j'}(\bar{y}_0)\,,\tag{2}$$

where $N=3^S$, $\{\bar{x}_0,\bar{y}_0\}=\left\{\frac{x_0}{a},\frac{y_0}{a}\right\}$ (being a the half-width of the zone plate and $\{x_0,y_0\}$ the cartesian coordinates at the pupil plane), and $RECT_j(x)$ is defined as

$$RECT_j(x)=\left[rect\left(\sqrt{\frac{N}{j}}\,x\right)-rect\left(\sqrt{\frac{N}{j-1}}\,x\right)\right].\tag{3}$$

In Eq. (3), $rect(x)$ is the rectangle function which takes the value 1 for $|x|\leq 1$ and 0 elsewhere. Thus, Fig. 1(c) shows a CDZP pupil of order $S=3$ in normalized coordinates.

3. Focusing properties

Under a monochromatic plane wave illumination, the diffracted irradiance patterns produced by a CDZP can be expressed (applying the Fresnel approximation) as:

$$I(\bar{x},\bar{y},u)=4u^2\left|\int_{-1}^{1}\int_{-1}^{1}q(\bar{x}_0,\bar{y}_0)\exp\left\{-2\pi iu\left[\left(\bar{x}_0^2+\bar{y}_0^2\right)-\left(2\bar{x}\bar{x}_0+2\bar{y}\bar{y}_0\right)\right]\right\}d\bar{x}_0d\bar{y}_0\right|^2,\tag{4}$$

#181234 - $15.00 USD Received 5 Dec 2012; revised 14 Jan 2013; accepted 14 Jan 2013; published 28 Jan 2013
(C) 2013 OSA

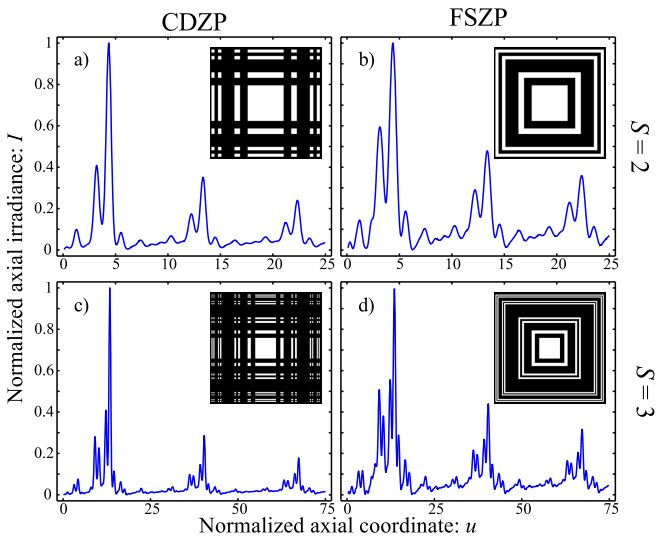

Fig. 2. Normalized axial irradiance for the CDZP and its associated FSZP.

where $u = a^2/2\lambda z$ is the normalized axial coordinate and $\{\bar{x},\bar{y}\} = \left\{\frac{x}{a},\frac{y}{a}\right\}$ are the normalized transverse coordinates. From the pupil function $q(\bar{x}_0,\bar{y}_0)$, defined in Eq. (2), it is easy to obtain the irradiance of a CDZP analytically:

$$I(\bar{x},\bar{y},u) = \frac{1}{16}\left|\sum_{j}^{N}\left\{\left[ERF_j(\bar{x},u) - ERF_{j-1}(\bar{x},u)\right] \times \sum_{j'}^{N} t_{Sjj'}\left[ERF_{j'}(\bar{y},u) - ERF_{j'-1}(\bar{y},u)\right]\right\}\right|^2, \tag{5}$$

where

$$ERF_j(x,u) = Erf\left[(1+i)\sqrt{\pi u}\left(\sqrt{\frac{j}{N}}+x\right)\right] + Erf\left[(1+i)\sqrt{\pi u}\left(\sqrt{\frac{j}{N}}-x\right)\right],$$

being $Erf[x] = 2\pi^{-1/2}\int_0^x \exp(-t^2)dt$ the error function. The irradiance along the optical axis, $\{\bar{x},\bar{y}\} = \{0,0\}$, Eq. (5) is:

$$I(0,0,u) = \left|\sum_{j}^{N} t_{Sjj}\left\{Erf\left[(1+i)\sqrt{\pi u}\sqrt{\frac{j}{N}}\right] - Erf\left[(1+i)\sqrt{\pi u}\sqrt{\frac{j-1}{N}}\right]\right\}\right|^4. \tag{6}$$

To compare the performance of a CDZP with the associated FSZP we used Eq. (6) to compute the axial irradiances. The result for $S = 2$ and $S = 3$ up to third order foci is shown in Fig. 2. It can be seen that CDZPs preserves the characteristic self-similar behavior of a FSZP with the foci located at the same positions because the axial patterns for $S = 3$ are a modulated version of that for $S = 2$. However, the secondary foci of CDZP are apodized with respect to FSZP ones. It can be also observed that the apodization is enhaced for higher fractal orders improving the diffraction efficiency.

4. Experimental results

The performance of different CDZPs have been tested experimentally with a programmable Liquid Crystal on Silicon SLM (Holoeye PLUTO, 8-bit gray-level, pixel size $d = 8\,\mu$m and

#181234 - $15.00 USD Received 5 Dec 2012; revised 14 Jan 2013; accepted 14 Jan 2013; published 28 Jan 2013
(C) 2013 OSA

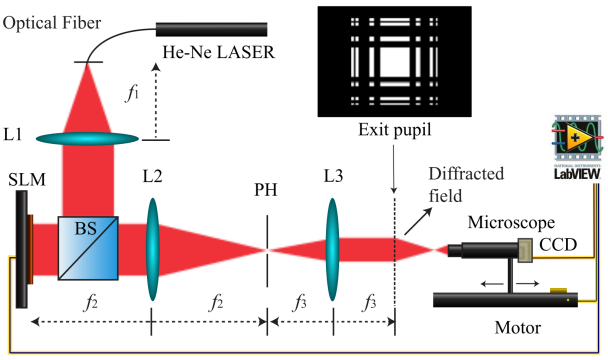

Fig. 3. Scheme of the experimental setup used for the simulation of the lenses.

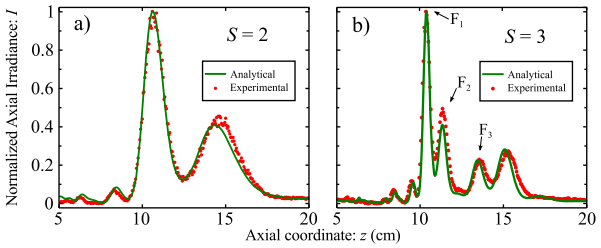

Fig. 4. a) Analytical (green) and experimental (red) irradiances provided by different fractal order CDZPs (first order focus) for $S = 2$. b) Same as in Fig. 4(b) for $S = 3$; F_1, F_2, F_3 are three different maxima of the compound first order focus. (see Fig. 5)

resolution equal to 1920×1080) operating in phase-only modulation mode. The SLM was calibrated for a 2π phase shift at $\lambda = 633\,\text{nm}$. The experimental setup is sketched in Fig. 3. A collimated beam (He-Ne Laser $\lambda = 633\,\text{nm}$) impinges onto the SLM, in which the CDZP is programed adding a linear phase grating to avoid the noise originated by the specular reflection (zero order diffraction) and the pixelated structure of the SLM (higher diffraction orders). This linear phase is compensated by tilting the SLM slightly and a pin-hole (PH) filter all diffraction orders except the order $+1$. Then at lens L3 focal plane (exit pupil) is a rescaled image of the desired lens pupile. The diffracted field is captured and registered with a microscope (4x Zeiss Plan-Apochromat objective) attached to a CCD camera (EO-1312M 1/2" CCD Monochrome USB Camera, 8-bit gray-level, pixel pitch of $4.65\,\mu\text{m}$ and 1280×1024 pixels). The microscope and the CCD are mounted on a translation stage (Thorlabs LTS 300, Range: 300 mm and $5\,\mu\text{m}$ precision) along the optical axis. The programming of the SLM, movements of the translation stage, the image recording and analysis is fully automatized by means of a LabVIEW program.

The experimental and the analytical axial irradiances are shown together in Fig. 4 for comparison. We have taken $a = 0.75\,\text{mm}$ and $1.31\,\text{mm}$ for $S = 2$ and $S = 3$ respectively in order to fix the main focus at the same position in both cases.

The distribution of the diffracted pattern over the whole transverse plane is of interest for the prediction of applications capabilities of CDZPs. Thus, a two-dimensional analysis of the diffracted irradiances is required. Equation (5) has been used to calculate the evolution of the diffraction patterns provided by a CDZP from near field to far field. Of particular interest are the irradiance patterns in the transverse planes which correspond to the different maxima of the axial irradiance.

In Fig. 5 the experimental transverse irradiances obtained at the main focus ($z = 10.4\,\text{cm}$) and

#181234 - $15.00 USD Received 5 Dec 2012; revised 14 Jan 2013; accepted 14 Jan 2013; published 28 Jan 2013
(C) 2013 OSA

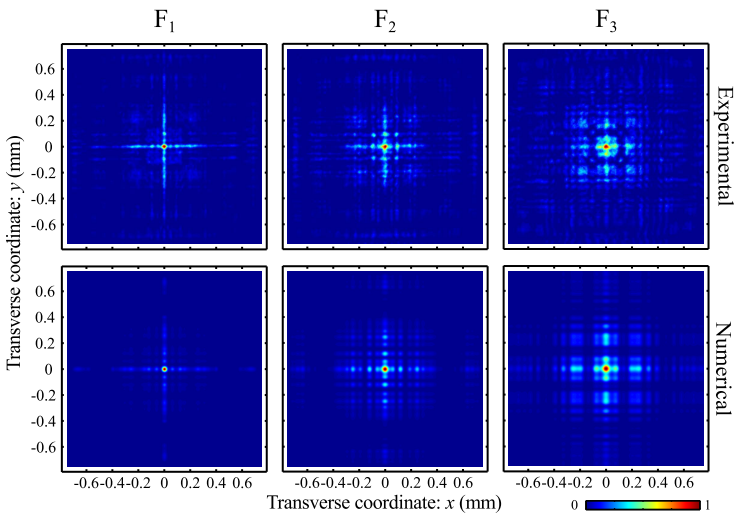

Fig. 5. Experimental transverse irradiance (top) compared with the analytically obtained irradiance (bottom) for a fractal order $S = 3$ CDZP. Transversal planes belong to the first order focus shown in Fig. 4(b) located at $z = 10.4$ cm and two secondary foci at $z = 11.3$ cm and $z = 13.6$ cm.

at two subsidiary foci ($z = 11.3$ cm and $z = 13.6$ cm) can be compared with the analytical results calculated using Eq. (5) for the order $S = 3$. In all cases, the irradiance has been normalized to its own maximum value. In spite of that the experimental images are affected by noise and by the aberrations of both, L3 and the microscope objective, a very good agreement with the numerical simulation is obtained. A characteristic two-arms-cross pattern at the main focus, extended to the subsidiary foci, can also be observed, so this behavior can be interpreted as an extension of depth of focus.

5. Conclusions

A new fractal diffractive optical element a CDZP is proposed. The focusing properties of this novel kind of lenses are analytically and experimentally investigated. The axial irradiances provided by these elements have been computed for different fractal stages obtaining a self-similar behavior. Moreover, under a monochromatic illumination, a CDZP gives rise a focal volume containing a delimited sequence of two-arms-cross patterns which are axially distributed according to the self-similarity of the lens. One potential application of CDZP is to generate a reference pattern in optical alignment and calibration of 3D systems. A spiral phase mask superposed to the CDZP pupil function —Eq. (2)— can be used for generating hollow rectangular beams [19]. Moreover, CDZP could be applied in THz communications given that Fresnel zone plates have been proved to be valuable elements for improving the performance in infrared antennas [20]. On the other hand, its cross-shaped focal pattern and its enhanced focal depth could be also helpful to perform parallel photopolymerisation in three-dimensional microstructure fabrication [21]

Acknowledgments

We acknowledge the financial support from Ministerio de Economía y Competitividad (grants FIS2011-23175 and TRA2009-0215), Generalitat Valenciana (grant PROMETEO2009-077), and Universitat Politècnica de València (PAID-05-11), Spain.